BJET
(Bayero Journal of Engineering and Technology)
https://bjet.ng/index.php/jet

Research Article
2026, Vol. 21 (1), 145-159

EVALUATION OF IMPACT RESISTANCE OF SELF-COMPACTING CONCRETE INCORPORATING RICE HUSK ASH AND RECYCLED POLYVINYL CHLORIDE (PVC) FIBRE

A. M. Nabade[1,2], J. M. Kaura[1], A. Ocholi[1], B. H. S. Amartey[1], I. Aliyu[1], I. Garba[1], M. Y. Sanni[3] and B. Sheriff[4]

[1]Department of Civil Engineering, Faculty of Engineering, Ahmadu Bello University Zaria, Nigeria
[2]Department of Civil Engineering, Faculty of Engineering, Kebbi State University of Science and Technology Aliero, Nigeria
[3]Nigerian Building and Road Research Institute (NBRRI), Jabi, Abuja, Nigeria
[4]Department of Civil Engineering, Ramat Polytechnic Maiduguri, Nigeria

*Corresponding author email: amnabade@gmail.com

Received: 22-04-2025
Revised: 22-09-2025
Accepted: 02-02-2026
Published: 08-04-2026

Abstract: *Concrete's brittle nature makes it highly vulnerable to severe damage or sudden collapse under impact loading scenarios. The integration of fibrous materials has proven to improve concrete's ductility, impact resistance and its overall performance. This study evaluate the impact resistance of self-compacting concrete (SCC) blended with eco-friendly materials from agricultural wastes; specifically rice husk ash (RHA) as partial cement replacement material and recycled polyvinyl chloride (PVC) water package as environmentally friendly sustainable polyethene fibre reinforcement (PFR). To achieve the desired objectives of this study, RHA was incorporated in SCC at six levels between 0 to 25%, while PFR was added at four levels between 0 to 1.5% by weight of cement. The absorbed impact energy (AIE) of polyethene fibre reinforced self-compacting concrete (PFRSCC) was assessed using drop weight test method on 384 cylindrical specimens (152mm diameter × 63.5mm high) following ACI 544.2R guidelines. The results revealed that PFRSCC significantly exhibited highest absorbed ultimate impact energy (AUIE) of 1307J, 2062.2J, 2410.7J and 2643.1J under respective curing periods of 7, 28, 56 and 90 days. The findings of this study conclude that PFR and RHA integration significantly enhance structural integrity of concrete under impact loading conditions. The study recommend optimal blend of 20% RHA and 1.5% PFR for maximum impact energy absorption under prolonged period, making PFRSCC a viable option for resilient structural concrete applications.*

Key words: Recycled PVC; drop weight method; absorbed impact energy; PFRSCC; polyethene fibre

1 Introduction

Despite extensive research on fibre-reinforced concrete (FRC), there is still a significant research gap in the use of eco-friendly and cost-effective solid-waste fibres, particularly recycled polyvinyl chloride (PVC) water sachets for enhancing the impact resistance of self-compacting concrete (SCC). Moreover, the synergistic use of recycled polyethene fibres with agricultural waste supplementary cementitious materials (SCMs) such as rice husk ash (RHA) has not been sufficiently explored. Most existing studies focus on conventional steel fibres or virgin synthetic fibres, with limited attention given to sustainable waste-derived alternatives that are capable of improving ductility and impact energy absorption.

Concrete is one of the most widely used structural materials due to its high compressive strength. However, its brittleness renders it vulnerable to sudden failure under impact loading (Smarzewski and Stolarski, 2022). The structural safety of concrete can be severely compromised under impact loading from vehicle collisions, falling objects and blast loads, as plain concrete exhibits low energy absorption capacity and limited crack resistance (Iman and Maryam, 2018; Elias *et al.*, 2018; Zhang *et al.*, 2021a).

Previous studies aimed at mitigating brittleness issues mostly focused on cementitious matrix modification through lightweight aggregates, SCMs and nano-scale additives. For example, Iman and Maryam (2018) reported reduced concrete's brittleness using expanded polystyrene particles, Elias *et al.*, (2018) demonstrated improved fracture toughness with RHA incorporation and Zhang *et al.*, (2021a) showed enhanced impact resistance through nano-silica-induced microstructural refinement. While the approaches by these researchers were found to improve crack control, matrix modification alone has been proven insufficient to prevent brittle failure under repeated or high-energy impact loading.

Consequently, fibre reinforcement has emerged as a more effective approach for improving impact performance of concrete. ACI 116R-00 (2000) defines fibre-reinforced concrete (FRC) as concrete incorporating randomly oriented discrete fibres to enhance one or more of its mechanical properties. However, numerous studies confirm that random dispersion of short fibres significantly improves post-cracking behaviour, toughness and energy dissipation, resulting in enhanced compressive, flexural and tensile strength as well as improved resistance to impact loading (Yoo and Banthia, 2018; Ahmad *et al.*, 2021; Kesavamoorthi and Ganesh, 2024).

Nowadays, steel fibres have been the most extensively studied due to their high tensile strength and crack-bridging efficiency. Yoo and Banthia (2018) attributed concrete performance enhancement primarily to fibre pull-out and crack-bridging mechanisms, while Zhang *et al.*, (2021b) demonstrated that steel fibres combined with nano-silica improved impact resistance and durability through fibre-matrix synergy. More recently, Kesavamoorthi and Ganesh (2024) showed that hybrid macro–micro steel fibre systems enhanced impact resistance and reliability of concrete structures via multi-scale crack arrest mechanisms. However, the application of steel fibres is constrained by high cost, corrosion susceptibility, increased density and environmental concerns (Zhang *et al.*, 2021b; Bakhshi *et al.*, 2024).

Synthetic fibres such as polypropylene and nylon offer improved durability and corrosion resistance. Ahmad *et al.*, (2021) reported improved toughness and impact resistance in nylon fibre-reinforced SCC; however, most studies rely on virgin polymers, raising sustainability and economic concerns (Awoyera *et al.*, 2022).

The impact resistance of FRC is commonly evaluated using repeated drop-weight test recommended in ACI 544.2R (1999) due to its simplicity and cost-effectiveness. Nevertheless, this method exhibits high variability and limited representation of real structural impact conditions, meaning that most studies report relative rather than absolute impact performance (ACI 116R-00, 2000). In comparison, the Charpy impact test provides rapid and repeatable measurements for small specimens, while the split-Hopkinson pressure bar test allows evaluation of impact resistance of concrete under high strain-rate conditions, offering more precise insights into dynamic material behaviour.

In view of the identified research gap, this study investigate the impact resistance of grade M30 self-compacting concrete incorporating rice husk ash and recycled PVC fibres, with the objective of enhancing impact energy absorption and ductility while promoting sustainable material utilization and effective solid-waste management.

2 Materials and Methods

2.1 Materials and their Test Methods

The materials used in this study include aggregates; cement as the primary binder; rice husk ash (RHA) as a partial cement replacement; polycarboxylate ether–based superplasticizer serving as a water-reducing admixture; and recycled polyvinyl chloride (PVC) water package used as polyethene fibre reinforcement (PFR). Clean water was used throughout for mixing of all concrete constituents.

The aggregates were characterized by fineness modulus (FM), specific gravity and density. Moreover, coarse aggregate was characterized by impact and crushing values (AIV and ACV). Tests on aggregates were carried out in accordance with the requirements of BS 882 (1992) and BS EN 12620 (2013).

Dangote Cement brand 3X (grade 42.5N) was procured from a local retail outlet in Zaria, while rice husks (RHs) were obtained from local rice processing mills within Zaria metropolis. The rice husk ash (RHA) was produced under controlled combustion of RHs in a muffle furnace at a temperature of 600°C for 4 hours. The resulting RHA was subsequently subjected to ball milling to achieve particles finer than cement, enabling its use as a supplementary cementitious material (SCM) in concrete. Based on the requirements of ASTM C618-08a (2008), the RHA was classified as a pozzolanic material, being its major oxide compounds (SiO_2+Al_2O_3+Fe_2O_3) > 70% and minor oxide compounds; MgO < 5%, Na_2O < 1.5% and SO_3 < 5%. Tests conducted on the cement included specific gravity, fineness, standard consistency, setting time and soundness. These physical properties were determined in accordance with EN 197-1 (2000), while the RHA was characterized through oxide composition, fineness and specific gravity tests.

Discarded PVC water sachets were collected from within and around the campuses of Ahmadu Bello University, Zaria. The sachets were thoroughly washed to remove impurities that could adversely affect concrete properties and then air-dried in the Concrete and Materials Laboratory of the Department of Civil Engineering, Ahmadu Bello University, Zaria. The dried sachets were subsequently shredded into fibres of uniform dimensions, measuring 15mm in width and 60mm in length. The thickness of the fibre was measured using a digital Vernier caliper as 0.2mm and hence its aspect ratio was computed as 300. The tensile properties of the recycled PVC fibres were determined in accordance with ASTM D3822 (2017) using a universal tensile testing machine at the Department of Polymer and Textile Engineering, Ahmadu Bello University, Zaria. During testing, PVC fibre was mounted between the machine grips using a low-capacity 50N load cell, with an initial gauge length of 25mm. Uniaxial tensile load was applied at a constant crosshead speed of 5mm/min until failure. Load and elongation were continuously recorded, from which the maximum tensile load, tensile strength, elongation at break and stress–strain behaviour were obtained from the load–displacement curves. Plates I to III illustrate the sourcing, processing and procedures for testing the PVC fibre reinforcement.

Plate I: PFRs (Discarded PVC waste)

Plate II: PFR under tensile test

Plate III: PFR's results processing

Table 1 presents the mix proportions of polyethene fibre-reinforced self-compacting concrete (PFRSCC) determined in accordance with EFNARC guidelines and the IS 10262 (2019) standard. The table includes 24 designed mix proportions for both SCC and PFRSCC.

Table 1: Mix Proportions of SCC and PFRSCC Mix*es*

Mixture Label	RHA (%)	PFR (%)	Cement (kg/m^3)	RHA (kg/m^3)	W/C Ratio	PFR (kg/m^3)	Water (kg/m^3)	SP (kg/m^3)	FA (kg/m^3)	CA (kg/m^3)
SCC (Control)	0	0	340	0	0.50	0	170	3.06	870	997
PFRSCC1	0	0.5	340	0	0.50	1.70	170	3.06	870	997
PFRSCC2	0	1.0	340	0	0.50	3.40	170	3.06	870	997
PFRSCC3	0	1.5	340	0	0.50	5.10	170	3.06	870	997
PFRSCC4	5	0	323	17	0.50	0	170	3.06	870	997
PFRSCC5	5	0.5	323	17	0.50	1.70	170	3.06	870	997
PFRSCC6	5	1.0	323	17	0.50	3.40	170	3.06	870	997
PFRSCC7	5	1.5	323	17	0.50	5.10	170	3.06	870	997
PFRSCC8	10	0	306	34	0.50	0	170	3.06	870	997
PFRSCC9	10	0.5	306	34	0.50	1.70	170	3.06	870	997
PFRSCC10	10	1.0	306	34	0.50	3.40	170	3.06	870	997

PFRSCC11	10	1.5	306	34	0.50	5.10	170	3.06	870	997
PFRSCC12	15	0	289	51	0.50	0	170	3.06	870	997
PFRSCC13	15	0.5	289	51	0.50	1.70	170	3.06	870	997
PFRSCC14	15	1.0	289	51	0.50	3.40	170	3.06	870	997
PFRSCC15	15	1.5	289	51	0.50	5.10	170	3.06	870	997
PFRSCC16	20	0	272	68	0.50	0	170	3.06	870	997
PFRSCC17	20	0.5	272	68	0.50	1.70	170	3.06	870	997
PFRSCC18	20	1.0	272	68	0.50	3.40	170	3.06	870	997
PFRSCC19	20	1.5	272	68	0.50	5.10	170	3.06	870	997
PFRSCC20	25	0	255	85	0.50	0	170	3.06	870	997
PFRSCC21	25	0.5	255	85	0.50	1.70	170	3.06	870	997
PFRSCC22	25	1.0	255	85	0.50	3.40	170	3.06	870	997
PFRSCC23	25	1.5	255	85	0.50	5.10	170	3.06	870	997

Note: RHA= Rice husk ash, PFR= polyethene fibre reinforcement, W/C= water to cement ratio, SP= superplasticizer, FA= fine aggregate, CA= coarse aggregate, SCC= self-compacting concrete, PFRSCC1 to PFRSCC23 represent mix with different percentage of RHA and PFR

2.2 Mixing of Constituents and Preparation of Specimens

The mixing of the constituent materials of PFRSCC mixes were carried out under laboratory conditions at an ambient temperature of approximately 20–25°C and relative humidity of 50–65% in accordance with ASTM C192/C192M (2019). These conditions were maintained to ensure stable rheological behaviour and uniform dispersion of PVC fibres in the self-compacting concrete.

The mixing commenced with finer materials (fine aggregate, cement and RHA). Thereafter, water was gradually added, after which; the coarse aggregate was added until homogeneous mixture was achieved, then PVC fibres were later added. Moreover, in order to improve and/or maintain workability and as well ensure homogeneity of the mixes, superplasticizer that was polycarboxylate ether-based was added at a dosage of 0.9% by weight of cement. A total number of 24 different mixes were prepared while maintaining average mixing time between 15 - 20 minutes for each mix containing varying blends of RHA and PVC fibre reinforcement.

The test specimens used for impact resistance evaluation consisted of 384 concrete cylinders cast from 24 different mixes of PVC fibre-reinforced self-compacting concrete, each with a diameter of 152 mm and a depth of 63.5 mm.

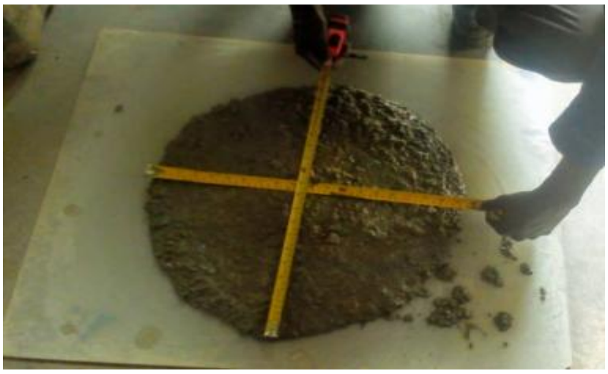

Plate IV: FA tests (SF + T_{500})

Plate V: PA test (L-box)

Plate VI. SR test (Wet sieving)

2.3 Test Methods for Workability

The workability properties of PFRSCC were characterized based on EFNARC (2002 & 2005) using three (3) important characteristics of SCC; filling ability (FA) tests (slump flow and T_{500} slump flow time), passing ability (PA) tests (L-box and J-ring) and segregation resistance (SR) tests (T_{5min} and wet sieving). Plates IV to VI show procedure on some categories of tests conducted on fresh characteristics of SCC and PFRSCC.

2.4 Test Methods for Impact Resistance

The impact resistance tests were performed on 384 concrete cylinders (152mm diameter×63.5mm high) using repeated drop weight test method, following ACI 544.2R (1999) guidelines. The tests were conducted at 7, 28, 56 and 90 days curing periods based on the following procedures:

i. The impact resistance was determined using 19.4kg hammer, that repeatedly dropped from a height of 18 inches (457mm) on 64.5mm diameter steel ball, positioned at the centre of cylindrical specimen (See Plate VIII).
ii. The number of repeated drops that produced the yield (first visible crack) was recorded. At the emergence of the yield, the repeated impact drops were continued until the specimen experienced complete (total) fracture, then the number of drops that caused the ultimate crack was also recorded.
iii. The time (t) required for the hammer to drop from the height of 18 inches and strike the 64.5mm diameter steel ball on the test specimens was computed from equation 1:

$$t = \sqrt{\frac{h}{0.5g}} \quad (1)$$

iv. The impact velocity (V) and absorbed impact energy (AIE) were computed from equations 2 and 3, as reported by researchers (Karthikeyan and Dhinakaran, 2018; Vivek *et al.*, 2023).

$$V = gt \quad (2)$$

$$AIE = \left(\frac{mV^2}{2}\right)n \quad (3)$$

Where the parameters; V, m, g, n, h, and E, represent impact velocity (m/s), mass of the hammer (kg), acceleration due to gravity (m/s^2), number of impact blows (dimensionless), dropping height of the hammer (m) and absorbed impact energy (J) respectively.

Plates VII to IX illustrate pictorial views of some stages involved in impact resistance evaluation.


Plate VII: Impact test assembly

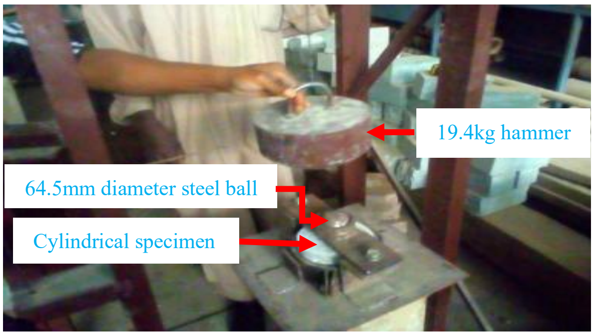

Plate VIII: Repeated drop weight test


Plate IX: Fractured test specimen

3 Results and Discussion

In this study, the effect of varying RHA and PFR (from 0 to 25%) and PFR (from 0 to 1.5%) as respective partial replacement material and fibre reinforcement on impact energy absorption capacity of structural PFRSCC were presented.

3.1 Materials Characteristics

Table 2 presents the results of properties of constituent materials (aggregates, cement, RHA and PFR) used to achieve the desired objective of the study.

Table 2: Characteristics of Constituent Materials

Description of test	Results	Limits/Range	Reference
Fine Aggregate (River Sand)			
Fineness modulus (FM)	2.95	2.30 - 3.10	IS 383 (2016)
Specific gravity	2.62	2.50 – 3.00	ASTM C128-22 (2022)
Density (kg/m^3)	1360	< 1520	BS EN 1097-6 (2000)
Water absorption (%)	1.07	1.06	BS EN 1097-6 (2000)
Coarse Aggregate (Crushed Granite)			
Fineness modulus (FM)	7.55	6.00 - 8.50	IS 383 (2016)
Specific gravity	2.71	2.50 - 2.80	ASTM C127-24 (2015)
Density (kg/m^3)	1475	1200 - 1600	BS EN 1097-6 (2000)
Water absorption (%)	0.3	0.1 – 4.0	BS EN 1097-6 (2000)
Aggregate impact value, AIV (%)	24.8	≤ 30	BS 812-110 (1990)
Aggregate crushing value, ACV (%)	21.4	≤ 30	BS 812-112 (1990)
Portland Limestone Cement (Major Binder)			
Specific gravity	3.14	3.10 - 3.16	BS EN 1097-3 (1998)
Consistency (%)	31	26 - 33	BS EN 196-3 (2016)
Initial setting time (min)	88	≥ 45	BS EN 196-3 (2016)
Final setting time (min)	167	≤ 600	BS EN 196-3 (2016)
Fineness: Retained on 75 micron sieve (%)	6	< 10	BS EN 196-6 (2019)
Soundness (mm)	10	≤ 10	BS EN 196-3 (2016)
Rice Husk Ash, RHA (Cement replacement material)			
Specific gravity	2.20		
Fineness: Passing 75 micron (%)	98	≤ 100	
Total oxides compounds (%)	75.4	≥ 70	ASTM C618 (2008)
Polyethene Fibre Reinforcement (PFR)			
Tensile stress (MPa)	18.80	≥ 10	Szlachetka *et al.,* (2021)
Elongation at break (%)	265	≥ 200	Szlachetka *et al.,* (2021)

The results presented in Table 2 indicate that the Portland limestone cement used in this study satisfied the requirements for mortar and concrete production, as evidenced by its standard consistency, initial and final setting times, soundness, specific gravity and fineness values of 31%, (88 and 167) minutes, 10mm, 3.14 and 6% respectively. The fine aggregate also met the required standards for mortar and concrete production, with specific gravity, bulk density and water absorption values of 2.62, 1360kg/m³ and 1.06% respectively. Similarly, the coarse aggregate satisfied suitability criteria based on its specific gravity, bulk density, aggregate crushing value (ACV) and aggregate impact value (AIV) of 2.71, 1475kg/m³, 21.4% and 22.8% respectively. In addition, both RHA and the polyethene fibre reinforcement (PFR) were found to meet the relevant requirements for use as a supplementary cementitious material and fibre reinforcement respectively.

Figure 1 illustrates the stress-strain curve describing the mechanical behaviour of polyethene fibre reinforcement (PFR) produced from discarded PVC water sachets.

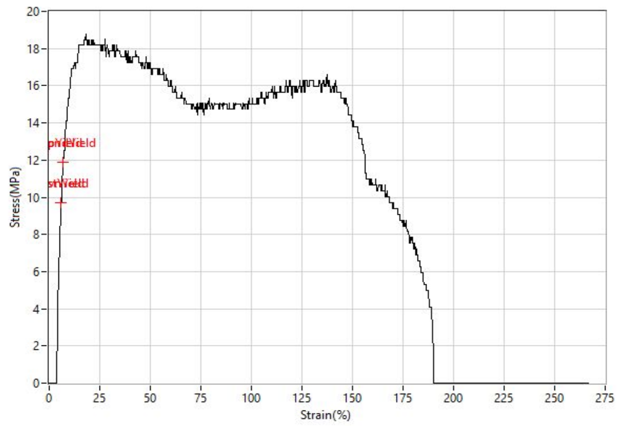

Figure 1: Polyethene fibre reinforcement (PFR's) stress-strain curve

The figure indicate that PFR exhibits low initial stiffness but high ductility. The initial linear region up to about 2–3% strain corresponds to an estimated Young's modulus of approximately 415MPa, while yielding occurs at around 10–12MPa. The fibre attained an ultimate tensile strength of roughly 18–19MPa at around 15–20% strain and sustains very large deformation before failure, with ultimate strain approaching around 180–200%. This combination of moderate tensile strength and exceptionally high elongation confirms the ductile nature of PFR, which is advantageous for crack bridging and energy

absorption under impact loading in fibre-reinforced concrete as reported by Yoo and Banthia (2018) and Zhang *et al.,* (2021a).
The Figure 1 also described the characteristic of strain hardening, during which molecular chain alignment and reorientation within PVC fibre enhance resistance to further deformation before softening occurs. After reaching a peak stress of approximately 18MPa, a slight stress reduction is observed, followed by a stable plateau between about 75% and 190% strain, indicating pronounced ductility and sustained load-carrying capacity. The final failure occurs at strain approaching 265%, which is consistent with the tensile response of fibre reported in recent studies by Baghous and Barsoum (2021) and Zhang *et al.,* (2021a).

3.2 Materials Characteristics

Table 3 summarizes the workability characteristics of PFRSCC mixes according to EFNARC guidelines. The slump flow (SF) values indicate that flowability, ranged from 715mm (SCC control) to 520mm. The results indicate that increasing RHA and PFR content progressively reduced workability, though PFRSCC1 to PFRSCC19 met EFNARC criteria for passing ability and segregation resistance, demonstrating good overall fresh characteristic performance.
In contrast, at higher RHA and PFR levels, improved impact resistance is achieved through enhanced crack bridging and energy absorption, but this is accompanied by reduced workability due to increased water demand and fibre-induced internal friction. However, mixes with ≥20% RHA and ≥1.0–1.5% PFR approaches EFNARC workability limits, indicating a clear trade-off between fresh-state flowability and hardened impact performance. Practically, excessive stiffness may hinder placement in congested or complex structural elements, leading to incomplete filling or fibre clustering, which can undermine the intended performance benefits. These findings confirm the existence of a rheological threshold and emphasize that practical implementation of PFRSCC requires performance-based optimization, balancing impact resistance gains with adequate workability through controlled replacement levels and admixture adjustment rather than maximizing RHA and PFR contents (EFNARC, 2005; Yoo & Banthia, 2018).

Table 3: PFRSCC Workability Characteristics as per EFNARC Guidelines

S/N	Mix label	RHA (%)	PFR (%)	Filling Ability		Passing Ability		Segregation Resistance	
				SFS (mm)	T_{500} (s)	L-box ratio	J-ring B_J (mm)	T_{5min} (sec)	SR ratio
1	SCC (Control	0	0	715	2.3	0.96	0.25	11.0	9.76
2	PFRSCC1	0	0.5	710	2.4	0.94	0.75	11.2	9.24
3	PFRSCC2	0	1.0	705	2.4	0.93	1.00	11.5	8.60
4	PFRSCC3	0	1.5	700	2.5	0.92	1.50	11.9	8.02
5	PFRSCC4	5	0	695	2.6	0.94	1.00	11.8	8.18
6	PFRSCC5	5	0.5	685	2.7	0.93	1.50	12.0	7.70
7	PFRSCC6	5	1.0	680	2.8	0.90	2.00	12.3	7.42
8	PFRSCC7	5	1.5	670	2.9	0.88	2.50	12.5	7.26
9	PFRSCC8	10	0	655	3.0	0.91	2.25	12.4	7.70
10	PFRSCC9	10	0.5	645	3.1	0.89	3.00	12.5	7.54
11	PFRSCC10	10	1.0	640	3.1	0.87	3.50	12.7	7.36
12	PFRSCC11	10	1.5	630	3.2	0.86	3.75	13.1	6.96
13	PFRSCC12	15	0	620	3.3	0.90	3.00	13.0	7.22
14	PFRSCC13	15	0.5	615	3.4	0.89	4.25	13.4	6.78
15	PFRSCC14	15	1.0	610	3.4	0.88	5.00	13.6	6.52
16	PFRSCC15	15	1.5	600	3.6	0.87	5.25	13.9	6.24
17	PFRSCC16	20	0	585	3.8	0.89	4.75	13.7	6.68
18	PFRSCC17	20	0.5	570	4.0	0.88	5.50	13.7	6.38
19	PFRSCC18	20	1.0	565	4.0	0.87	6.00	14.0	6.04
20	PFRSCC19	20	1.5	550	4.2	0.85	6.75	14.2	5.62
21	PFRSCC20	25	0	540	4.3	0.83	6.00	13.8	6.42
22	PFRSCC21	25	0.5	530	4.4	0.82	7.50	14.0	6.08
23	PFRSCC22	25	1.0	525	4.5	0.81	9.00	14.3	5.66
24	PFRSCC23	25	1.5	520	4.7	0.82	9.75	14.7	5.24
EFNARC (2002 & 2005) Limits				SFS: 550-850mm	T_{500}: 0 - 5 sec	L-Box Ratio: 0 - 1.00	B_J: 0-10mm	T_{5min}: 11-15 sec (+3 sec)	SR: 5 - 15%

Note: RHA= Rice husk ash, PFR= polyethene fibre reinforcement, SCC= self-compacting concrete, PFRSCC1 to PFRSCC23 represent polyethene fibre reinforced concrete with different percentage of RHA and PFR

3.3 Effect of RHA and PFR on Repeated Impact

Figures 2 to 5 depicts the effects of RHA and PFR blend on the frequency of strikes (impact blows) that emerged first visible fracture (yield) and total fracture (ultimate) of structural PFRSCC under short and long-term concrete curing periods (7, 28, 56 and 90 days). From Figures 2 to 5, the general trend of the results indicated that the resistance of impact specimens to impact blows increases with increase in RHA substitution and PFR addition for SCC and PFRSCC1 (0% RHA and 0.5% PFR) to PFRSCC19 (20% RHA and 1.5% PFR), and then eventually declined for PFRSCC20 to PFRSCC23 . Reference to Figures 2 to 5, it can be observed that SCC (control mix) sustained the least number of blows for yield crack (NBYC) and the number of blows for ultimate cracks (NBUC) than PFRSCC mixes.

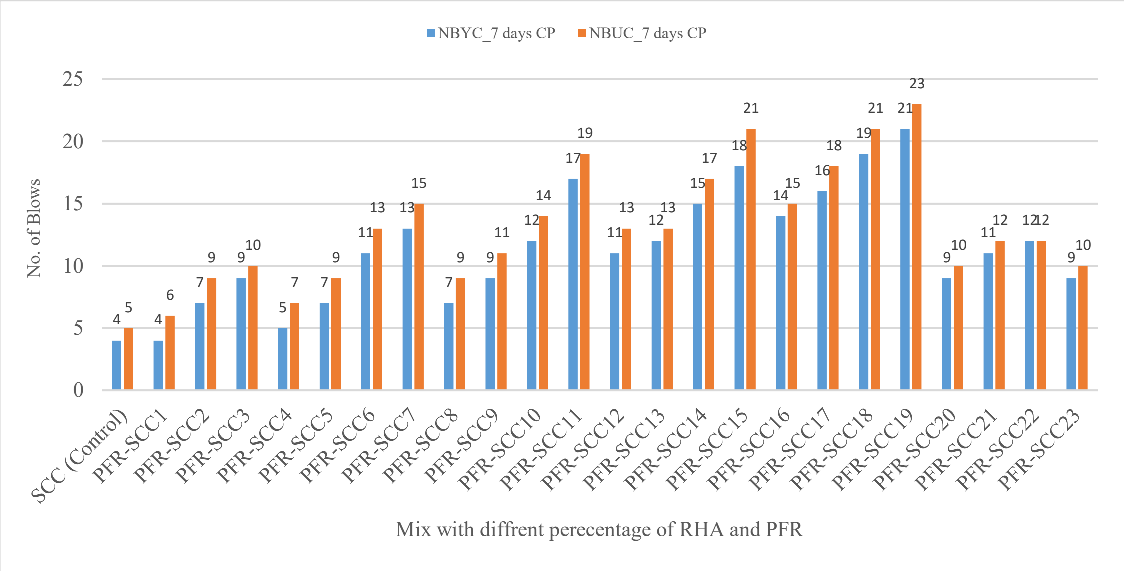

Figure 2: Impact blows responsible for yield (first) crack and ultimate crack for PFRSCC mixes (7 days curing period)

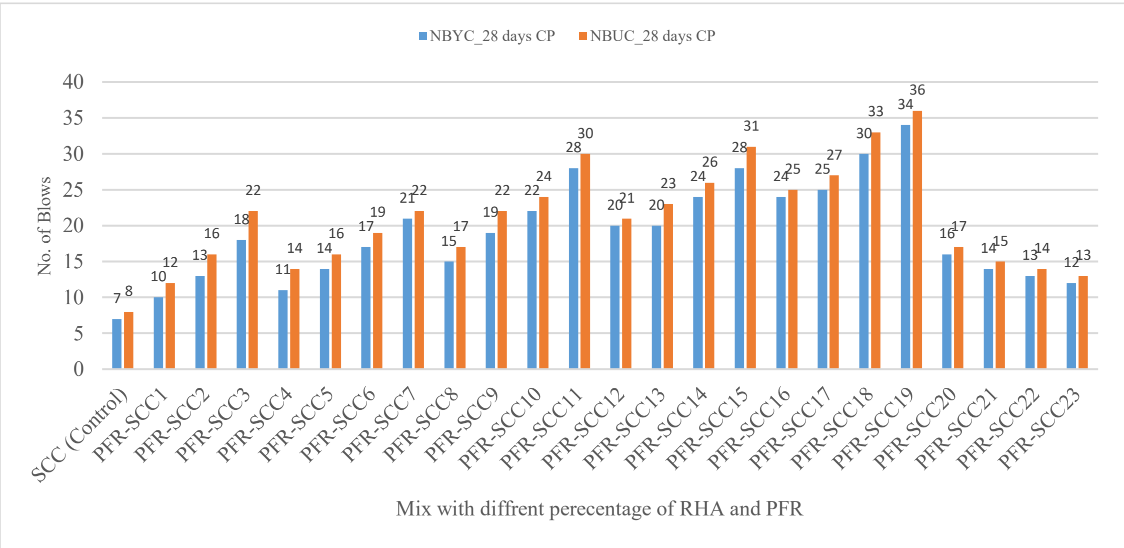

Figure 3*:* Impact blows responsible for yield (first) crack and ultimate crack for PFRSCC mixes (28 days curing period)

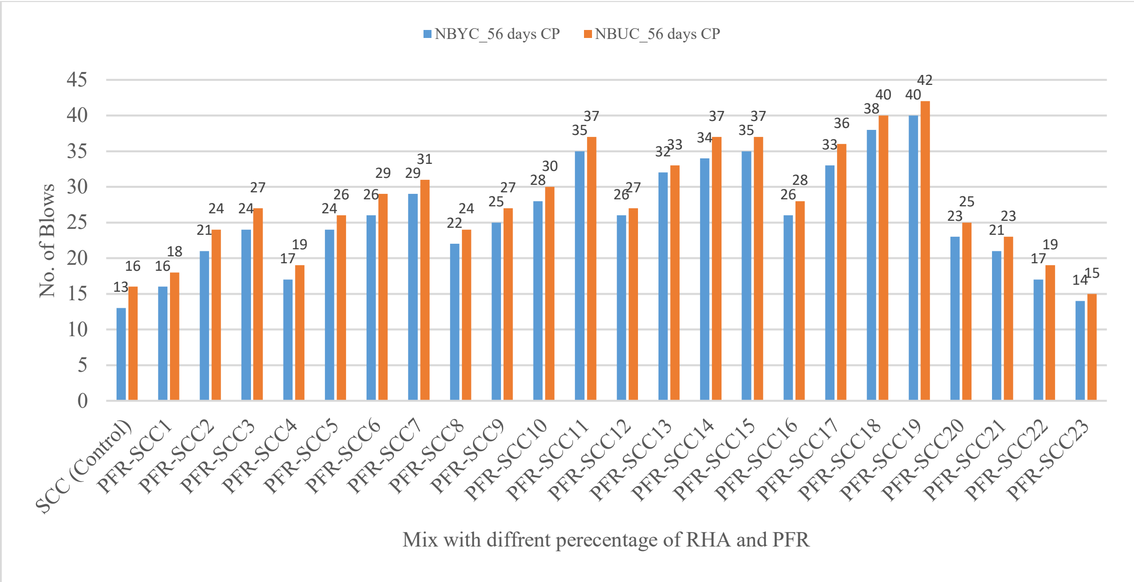

Figure 4: Impact blows responsible for yield (first) crack and ultimate crack for PFRSCC mixes (56 days curing period)

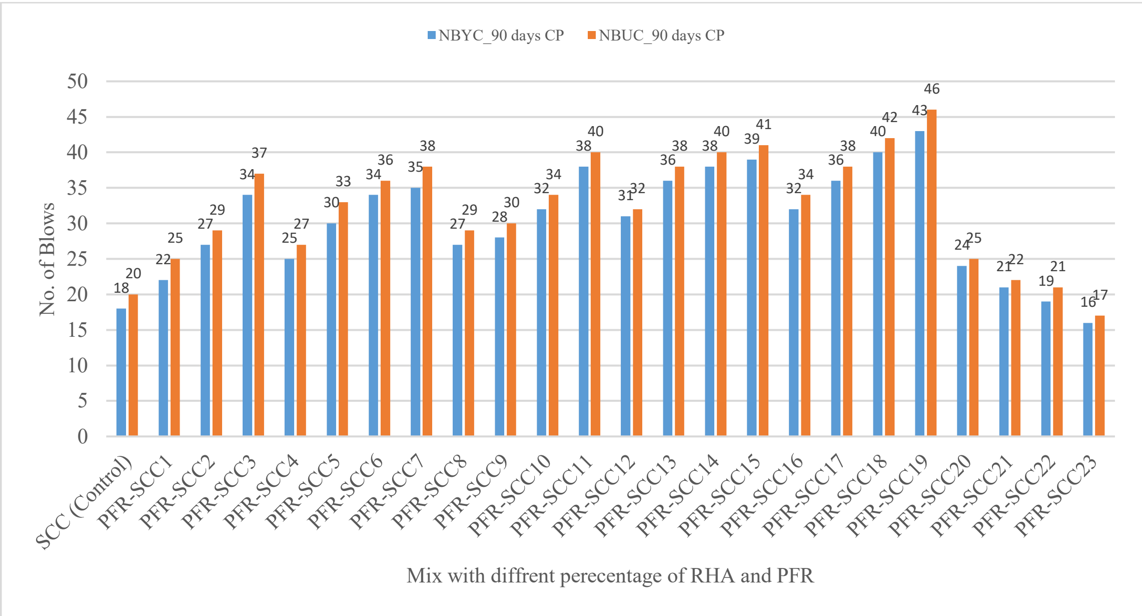

Figure 5: Impact blows responsible for yield (first) crack and ultimate crack for PFRSCC mixes (90 days curing period)

3.3.1 Stress Distribution Sequence of PFRSCC

Under impact loading, induced localized stress concentrate beneath the impactor (steel ball), generating compressive stress waves that propagated through the specimens and reflected as tensile stresses at the boundaries. These tensile stresses had governed the crack initiation, which occurred mainly at mortar-aggregate interfaces. The SCC control mix exhibited limited stress redistribution capacity, and hence these generated cracks quickly blended into a single dominant diametric crack causing brittle failure. For PFRSCC specimens, pores were refined with RHA, while PVC fibres bridges these cracks, distribute stresses and promote multiple fine cracks, resulting in ductile failure with high energy absorption capacity as reported by Coviello *et al.* (2024).

3.3.2 Crack Propagation in PFRSCC

Plates X and XI present respective test specimens before and after impact loading, indicating distinct crack initiation and failure characteristics among mixes. It was observed in plate XI that control SCC specimen exhibited rapid radial crack propagation, resulting in sudden brittle failure accompanied by extensive spalling and fragmentation. The number of blows required to initiate the first visible crack (NBYC) for the control mix was 4, 7, 13 and 18 at curing ages of 7, 28, 56 and 90 days respectively (See Figures 2 to 5). Ultimate failure (NBUC) followed shortly thereafter at 5, 8, 16 and 20 blows, confirming the limited post-cracking resistance and low energy absorption capacity of control SCC.

Plate X: SCC/PFR-SCC Specimens (Before Impact Blows)

Plate XI: SCC/PFR-SCC Specimens (After Impact Blows Showing Different Failure Modes)

In contrast, the PFRSCC specimens demonstrated delayed crack initiation and a more gradual crack propagation process, enabling progressive energy dissipation over repeated impacts. This improvement was observed to be most pronounced in the optimal mix (PFRSCC19), which recorded substantially higher NBYC values of 21, 34, 40 and 43 blows at 7, 28, 56 and 90 days respectively. The corresponding NBUC values of 23, 36, 42 and 46 blows were also observed (See Figures 2 to 5 and Plate XI), indicating a clear transition from brittle to ductile failure behaviour. Similar ductile response patterns in fibre-reinforced cementitious composites have been reported by Vivek *et al.*, (2023).

The post-impact examination of the failed specimens (Plate XI) further clarified these differences in fracture behaviour. The control SCC specimens failed in an explosive manner, breaking into large fragments with severe spalling, which is the characteristic of brittle fracture and low fracture toughness. Conversely, PFRSCC specimens exhibited a more uniformly distributed cracking, with visible fibre pull-out and reduced fragmentation, indicating effective crack-bridging and enhanced energy absorption capacity. Among all mixes, PFRSCC19 displayed the most stable failure mode, retaining greater structural integrity and exhibiting minimal spalling even after ultimate failure.

However, a closer inspection of crack patterns revealed a clear shift in fracture mechanics with the incorporation of PFR and RHA. The control SCC specimen showed a single dominant diametric crack with an estimated width of approximately 3.5mm, reflecting brittle splitting and limited post-impact resistance. In contrast, PFRSCC specimens developed multiple distributed cracks (typically 3–6 cracks per specimen) with significantly reduced crack widths in the range of 0.5–1.5 mm. This represents an approximate 50–70% reduction in crack width, providing quantitative evidence of improved ductility and post-impact integrity due to fibre crack-bridging. Consequently, specimens containing higher RHA contents (e.g. 25% RHA with 0.5% PFR) still exhibited distributed cracking but with slightly wider crack widths of about 1.5–2.0 mm. This suggests that excessive RHA content may marginally reduce matrix toughness, although the presence of fibres continues to effectively control crack propagation. Overall, the increased crack multiplicity and reduced crack widths observed in PFRSCC confirm a transition from brittle fracture to a more ductile, energy-absorbing failure mode, which is consistent with a fracture behaviour reported by Sobuz *et al.*, (2022).

3.3.3 Influence of RHA and PVC on PFRSCC

The addition of RHA and PVC fibres changed the failure pattern from brittle to ductile. The control SCC failed abruptly with a single dominant crack and severe spalling, while PFRSCC showed delayed cracking, multiple finer cracks, and fibre pull-out, leading to higher failure thresholds and improved energy absorption.

The enhanced resistance to impact blows for PFRSCC specimens is attributed to the synergistic effects of RHA and recycled PVC fibres. The pozzolanic activity and fine particle sizes of RHA refined the pore structure, reduced void connectivity and produced a denser cement matrix; thereby delaying crack initiation and propagation. Similar microstructural improvements due to RHA incorporation in SCC have been reported by Endale *et al.* (2022), Muhammad and Thienel (2023) and Plando and Maquiling (2023). Furthermore, the PVC fibres bridged developing cracks, restricted crack opening and dissipated impact energy through fibre deformation and pull-out, enabling specimens to sustain higher numbers of impact blows. This fibre-bridging mechanism aligns with the findings of Kesavamoorthi and Ganesh (2024). However, beyond the optimal composition (PFRSCC20 to PFRSCC23), the reduction in impact resistance was observed, which could be due to reduced workability and compromised self-compactability.

The overall results demonstrate that the optimal combination of 20% RHA and 1.5% PVC fibres (PFRSCC19) enhanced impact resistance by approximately 80–130% relative to the control SCC, highlighting the effectiveness of these sustainable materials in improving the toughness and impact performance of self-compacting concrete.

3.4 Absorbed Impact Energy

Figure 6 illustrates how absorbed yield impact energy (AYIE) and absorbed ultimate impact energy (AUIE) of PVC fibre-reinforced self-compacting concrete (PFRSCC) varied over curing periods of 7, 28, 56, and 90 days. The absorbed impact energy values were obtained by converting the recorded number of impact blows (shown in Figures 2 to 5) into corresponding impact energies. Both AYIE and AUIE increased steadily with curing age, indicating a continual improvement in the ability of PFRSCC to absorb impact energy as it matured. In contrast, the control self-compacting concrete (SCC) mix consistently absorbed the least energy, while all mixes incorporating rice husk ash (RHA) and PVC fibres showed remarkable improvement.

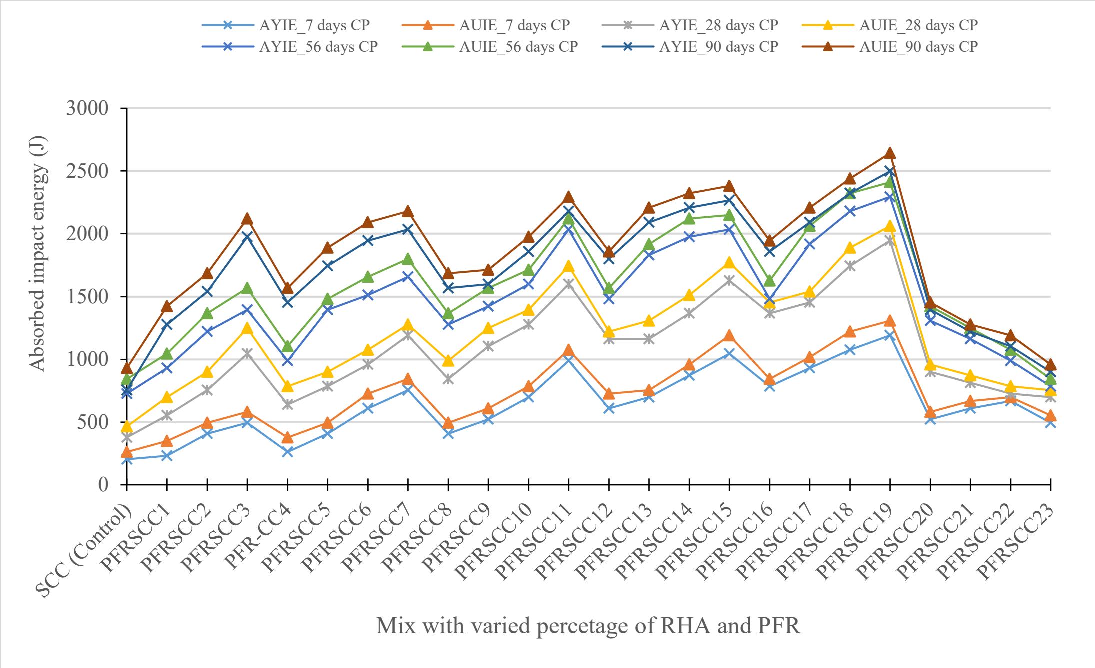

Figure 6: Absorbed Impact Energy Variation against Mix with Different Percentage of RHA and PFR

3.4.1 Impact Resistance Performance

3.3.1.1 ANOVA Results on Impact Resistance

A two-way ANOVA evaluated the effects of the 24 mixes and curing ages (7, 28, 56 and 90 days) on absorbed yield impact energy (AYIE) and ultimate impact energy (AUIE). Both factors showed statistically significant effects ($p<0.05$). Based on the statistical significance, PFRSCC consistently outperformed control SCC across all curing ages, with extended curing further enhancing yield and ultimate impact resistance.

3.3.1.2 ANOVA Results on Impact Resistance

From Figure 6, it was observed that the absorbed impact energy increases with PFR and RHA content, from approximately 232J (PFRSCC1) to a peak value of 2643J (PFRSCC19: 20% RHA+1.5% PFR). Beyond this optimum level, the energy absorption declined to approximately 1452J (PFRSCC20) and 958J (PFRSCC23), indicating that excessive RHA reduces matrix toughness despite the integration of fibres. This reflects the balance between effective crack-bridging by fibres and matrix cohesion under repeated impacts.

These results align with recent studies indicating that PVC fibres delay crack initiation, promote distributed cracking and boost impact energy absorption, while RHA enhance matrix densification and long-term strength (Danar *et al.*, 2020; Farhad *et al.*, 2020; Vijaya-Kumar *et al.*, 2022; Vivek *et al.*, 2023; Kesavamoorthi & Ganesh, 2024). Like Farhad *et al.* (2020), the optimal fibre–SCM proportions maximized resistance, but excess SCM marginally reduced toughness. The findings demonstrate a synergistic effect of RHA and PVC fibres, improving SCC's impact resistance, ductility and post-impact integrity within optimal proportions.

3.4.2 Energy Absorption Mechanisms

The combined effect of PVC fibres and RHA contributed to enhanced energy absorption for

PFRSCC under impact, reducing visible rupture and disintegration as compared with the control mix. This enhancement can be explained by the synergistic action of both materials, which helps delay crack initiation and slow down its propagation (Vivek *et al*., 2023). According to Sobuz *et al*. (2022), micro-cracks at the mortar–aggregate interface are regarded as the inherent weak points in concrete; however, incorporating fibres bridges these cracks, improving the integrity and toughness of the matrix.

3.4.3 Effect on Brittleness and Impact Resistance

In addition to improving impact energy absorption, fibre inclusion reduce the brittleness of the composite, confirming the earlier observations of Kumar *et al.* (2017) and Vivek *et al.* (2023). Kesavamoorthi and Ganesh (2024) also reported that fibres can raise concrete's impact strength at the yield and ultimate stages by roughly 50 - 200 % and 87 - 240 % respectively. In consistent with these studies, the results show that PFRSCC absorbed greater short- and long-term impact energies than the control SCC. Specifically, PFRSCC exhibited absorbed impact energies of 203.3 J and 261.4 J (7 days), 377.6 J and 464.7 J (28 days), 726.1 J and 842.3 J (56 days), and 755.2 J and 929.4 J (90 days).

These results indicated that PFRSCC absorbs significantly higher impact energies than control SCC across all curing ages, reflecting enhanced toughness, ductility and delayed crack propagation due to synergistic effect of PVC fibre and RHA. This progressive increase in impact resistance with curing age highlights improved matrix strength and fibre-matrix interaction over time.

This suggests practical applicability of PFRSCC in structural elements subjected to dynamic or sudden loads, such as industrial floors, slabs, barriers and protective structures. However, despite being a relative measure, the drop-weight results demonstrate that PFRSCC can better withstand real-world impact conditions than conventional SCC.

4 Conclusions

In this study, the influence of RHA and PFR on impact energy absorption capacity of structural PFRSCC were analyzed and discussed based on experimental results obtained using drop weight repeated impact tests. Based on the experimental findings, the following conclusions were drawn:

i. Determination of optimal levels of RHA and PFR provide a balance between workability and impact energy absorption capacity of structural PFRSCC.
ii. The integration of RHA and PFR has more influence on resistance of impact blows on structural PFRSCC than SCC (control mix).
iii. The high impact blows have positive influence on impact energy absorption capacity of structural PFRSCC than traditional concrete especially under prolonged period.
iv. An optimal blend of 20% RHA and 1.5% PFR provide maximum fracture energy performance of PFRSCC under short and prolonged periods, while promoting waste recycling.
v. Despite being a relative measure, the results of drop-weight absorbed impact energy of PFRSCC can better withstand real-world impact conditions than conventional SCC.

4.1 Recommendation for further research

Future studies should incorporate digital image analysis or crack-width microscopy to directly measure crack width evolution and fracture surface area for more precise quantification.

5 References

ACI 116R-00 (2000). Cement and Concrete (C & M) Terminology. Reported by ACI Committee 116. American Concrete Institute, 73p.

ACI 544.2R - 89, (1999). Measurement of properties of fiber reinforced concrete. Reported by ACI Committee 544. Manual of Concrete Practice, pp.1-12.

Ahmad, J., Zaid, O., Aslam, F., Martínez-García, R., Alharthi, Y.M., EI Ouni, M.H., Tufail, R.F. and Sharaky, I.A. (2021). Mechanical properties and durability assessment of nylon fiber reinforced self-compacting concrete. *Journal of Engineered Fibers and Fabrics, 16*, pp.1-13.

Anas, M., Khan, M., Bilal, H., Jadoon, S. and Khan, M.N. (2022). Fibre reinforced concrete: A review. *Engineering Proceedings, 22*, *3*, pp.1-7.

ASTM C128-22 (2022). Standard Test Method for Relative Density (Specific Gravity) and Absorption of Fine Aggregate. American Standard for Testing and Materials (ASTM), United State of America (USA).

ASTM C618-08a (2008). Standard Specification for Coal Fly Ash and Raw or Calcined Natural Pozzolan for Use in Concrete. Annual Book of ASTM Standards. American Society for Testing & Materials, USA.

ASTM C127-24 (2015). Standard Test Method for Relative Density (Specific Gravity) and Absorption of Coarse Aggregate. American Standard for Material and Testing (ASTM), USA.

ASTM D3822 (2017). Standard Test Method for Tensile Properties of Single Textile Fibers. American Standard for Material and Testing (ASTM), USA.

ASTM C192/C192M (2019) – Standard Practice for Making and Curing Concrete Test Specimens in the Laboratory. American Standard for Material and Testing (ASTM), USA.

Awoyera, P. O., Effiong, J. U., Olalusi, O. B., Arunachalam, K. P., de Azevedo, A. R. G., Martinelli, F. R. B. and Monteiro, S. N. (2022). Experimental findings and validation on torsional behaviour of fibre-reinforced concrete beams: A review. *Polymers, 14*, *1171*, pp.1-30.

Baghous, N. & Barsoum, I. (2021). Effect of material strength on ductile failure of steel in pressure vessel design. *Journal of Pressure Vessel Technology (JPVT), 143, 021503*, pp.1-14.

Bakhshi, M., Valente, I. B. and Ramezansefat, H. (2024). New model for evaluating the impact response of steel fiber reinforced concrete subjected to the repeated drop-weight. *Construction and Building Materials, 449, 138459*, pp.1-15.

BS 812-110 (1990). Testing Aggregates: Methods for Determination of Aggregate Crushing Value (ACV). European Committee for Standardization (CEN), Brussels, Belgium.

BS 812-112 (1990). Testing Aggregates: Methods for Determination of Aggregate Impact Value (AIV). European Committee for Standardization (CEN), Brussels, Belgium.

BS 882 (1992). Specification for aggregates from natural sources for concrete. European Committee for Standardization (CEN), Brussels, Belgium.

BS EN 197-1 (2000). Cement: Compositions, Specifications and Performance Criteria. European Committee for Standardization, CEN, Brussels.

BS EN 12620 (2013). Aggregates for Concrete (English Version). European Committee for Standardization, CEN, Brussels.

BS EN 196-3 (2016). Cement: Setting Time and Soundness (English Version). European Committee for Standardization, CEN, Brussels.

BS EN 196-6 (2019). Method for Testing Cement: Determination of Fineness (English Version). European Committee for Standardization, CEN, Brussels.

BS EN 1097-6 (2000). Tests for Mechanical and Physical Properties of Aggregates. Part 6: Determination of Particle Density and Water Absorption. British Standard Institution, London.

Coviello, C.G., Scala, A.L., Sabbà, M. F. & Carnimeo, L. (2024). On the cementitious mixtures reinforced with waste polyethene terephthalate. *Materials, 17, 5351*, pp.1-26. https://doi.org/10.3390/ma17215351

Danar, A., Dillshad, K. H. B. and Stefan, L. (2020). Mechanical properties and load deflection relationship of polypropylene fiber reinforced self-compacting lightweight concrete. *Construction Building Material Journal, 252*, 119084.

EFNARC (2002). The European Guidelines for Self-Compacting Concrete. Association House, 99 West Street, Farnham, Surrey GU9 7EN, UK. Available online at www.efnarc.org

EFNARC (2005). The European Guidelines for Self-Compacting Concrete. Association House, 99 West Street, Farnham, Surrey GU9 7EN, UK. Available online at www.efnarc.org

Endale, S. A., Taffese, W. Z., Vo, D. and Yehualaw, M. D. (2022). Rice Husk Ash in Concrete: Review. *Sustainability, 15, 137*, pp.1-26. https://doi.org/10.3390/su15010137

Elias, M. R., Javad, V. A. and Mohammad, R. D. (2018). Influence of rice husk ash on the fracture characteristics and brittleness of self-compacting concrete. *Engineering Fracture Mechanics, 199*, pp.595-608.

Farhad, A., Fatemeh, H., Afsaneh, V. and Anthony, T. D. (2020). High-performance fibre-reinforced heavyweight self-compacting concrete: Analysis of fresh and mechanical properties, Construction *Building Material Journal*, 232, 117230.

Greb, C., Lenz, C., Lengersdorf, M. & Gries, T. (2018) .Fabrics for reinforcement of engineering composites. In M. Menghe & H. X. John (Eds). Engineering of high performance textiles: The textile institute book series (pp.489-512).

Iman, M. N. and Maryam, G. (2018). The effect of expanded polystyrene synthetic particles on the fracture parameters, brittleness and mechanical properties of concrete. Theoretical Applied Fracture Mechanics, 94, pp.160-172.

IS 383 (2016). Specification for Coarse and Fine Aggregate for Concrete (Third Revision). Bureau of Indian Standards (BIS), New Delhi, India.

IS 10262 (2019). Concrete mix proportioning guidelines (2nd Edition). Bureau of Indian Standards (BIS), New Delhi, India, 40p.

Karthikeyan, B. & Dhinakaran, G. (2018). Influence of ultrafine TiO2 and silica fume on performance of unreinforced and fiber reinforced concrete, *Journal of Construction Building Material, 161*, pp.570-576.

Kesavamoorthi, R. and Ganesh, G. M. (2024). Impact resistance of macro and micro steel fibre reinforced self-compacted concrete (SFRSCC) with modelling and reliability analysis. *Discover Applied Sciences, 6(17)*, pp.3-16.

Kumar, A., Pratibha, N. and Tiwari, S. G. (2017). Performance of micro steel polypropylene fiber reinforced concrete under impact load. *Ind. Concrete Journal, 91(9)*, pp.25-29.

Luo, X., Sun, W. & Chan, Y.N. (2000). Characteristic of high performance steel fiber reinforced concrete subject to high velocity impact. Journal Cement & Concrete Research, 30(6), pp.907-914.

Mehrabi, P., Dackermann, U., Siddique, R. & Rashidi, M. (2024). A review on the effect of synthetic fibres, including macro fibres, on the thermal behaviour of fibre-reinforced concrete. *Buildings Journal, 14, 4006*, pp.1-30. https://doi.org/10.3390/buildings14124006

Muhammad, A. and Thienel, K. (2023). Properties of self-compacting concrete produced with optimized volumes of calcined clay and rice husk ash – Emphasis on rheology, flowability retention and durability. *Journal of Materials, 16, 5513*, pp.1-28.

Plando, F. R. P. and Maquiling, J. T. (2023). Microstructural characterizations and strength development of self-compacting concrete using rice husk ash. *Romanian Journal of Physics, 68, 908*, pp.1-9.

Ramasamy, S., Deivasigamani, V., Soundararajan, E. K. and Sridhar, J. (2024). Influence of nano silica on impact resistance and durability of fly ash concrete in structural buildings. *REVISTAMATERIA, 29(1)*, pp.1-14.

Smarzewski, P. and Stolarski, A. (2022). Properties and performance of concrete materials and structures. *Crystals, 12, 1193*, pp.1-5.

Sobuz, M. H. R., Saha, A., Anamika, J., Houda, M., Azab, M., Akid, A. S. M. and Rana, M. J. (2022). Development of self-compacting concrete incorporating rice husk ash with waste galvanized copper wire fiber. *Journal of Buildings, 12*, pp.1-23.

Szlachetka, O., Witkowska-Dobrev, J., Baryła, A. and Dohojda, M. (2021). Low-density polyethene (LDPE) building films – Tensile properties and surface morphology. *Journal of Building Engineering, 44, 103386*, pp.1-16.

Vijaya-Kumar, S., Deankumar, B. and Swami, B.L.P. (2022). Mathematical model for the impact strength of triple-blended steel fiber self-compacting concrete based on the experimental study, *Materials Today Proceedings. 60,* pp.576-581.

Vivek, S. S., Karthikeyan, B., Bahrami, A., Selvaraj, S. K., Rajasakthivel, R. & Azab, M. (2023). Impact & durability properties of alccofine-based hybrid fibre-reinforced self-compacting concrete. *Journal of Case Studies in Construction Materials, 19*, pp.1-16. www.elsevier.com/locate/cscm

Yoo, D. Y. and Banthia, N. (2018). Mechanical properties of ultra-high-performance fiber-reinforced concrete: A review. *Cement and Concrete Composites*, 73, pp.267-280.

Zhang, S., Han, B., Xie, H., An, M., & Lyu, S. (2021). Brittleness of concrete under different curing conditions. *Materials, 14, 7865*, pp.1-31. https://doi.org/10.3390/ma14247865

Zhang, P., Sha, D., Li, Q., Zhao, S. and Ling, Y. (2021a). Effect of nano silica particles on impact resistance and durability of concrete containing coal fly ash. *Nanomaterials, 11, 1296*, pp.1-18.

Zhang, P., Zhang, H., Cui, G., Yue, X., Guo, J. and Hui, D. (2021b). Effect of steel fiber on impact resistance and durability of concrete containing nano-SiO2. *Nanotechnology Reviews, 10,* pp.504-517.